What Kind of Initial Errors Cause the Severest Prediction Uncertainty of El Niño in Zebiak-Cane Model

XU Hui (徐 辉) and DUAN Wansuo* (段晚锁)

State Laboratory of Numerical Modeling for Atmospheric Sciences and Geophysical Fluid Dynamics (LASG),

Institute of Atmospheric Physics, Chinese Academy of Sciences, Beijing 100029

ABSTRACT

With the Zebiak-Cane (ZC) model, the initial error that has the largest effect on ENSO prediction is explored by conditional nonlinear optimal perturbation (CNOP). The results demonstrate that CNOP-type errors cause the largest prediction error of ENSO in the ZC model. By analyzing the behavior of CNOP-type errors, we find that for the normal states and the relatively weak El Niño events in the ZC model, the predictions tend to yield false alarms due to the uncertainties caused by CNOP. For the relatively strong El Niño events, the ZC model largely underestimates their intensities. Also, our results suggest that the error growth of El Niño in the ZC model depends on the phases of both the annual cycle and ENSO. The condition during northern spring and summer is most favorable for the error growth. The ENSO prediction bestriding these two seasons may be the most difficult. A linear singular vector (LSV) approach is also used to estimate the error growth of ENSO, but it underestimates the prediction uncertainties of ENSO in the ZC model. This result indicates that the different initial errors cause different amplitudes of prediction errors though they have same magnitudes. CNOP yields the severest prediction uncertainty. That is to say, the prediction skill of ENSO is closely related to the types of initial error. This finding illustrates a theoretical basis of data assimilation. It is expected that a data assimilation method can filter the initial errors related to CNOP and improve the ENSO forecast skill.

1. Introduction

The El Niño-Southern Oscillation (ENSO) phenomenon is one of the remarkable climate variations on the short-range climatic timescale ranging from a few months to several years. A milestone in ENSO forecasting was made after the development of Zebiak and Cane (1987) model (thereafter ZC model). The model predicted the development of positive sea surface temperature anomalies (SSTA) in the tropical Pacific one-year in advance of the onset of the 1986–87 El Niño event (Cane et al., 1986). Since then, numerous models have been developed to simulate ENSO. These models range from simple analytical ones (Battisti and Hirst, 1989; Wang and Fang, 1996; Jin, 1997) and intermediate coupled numerical models (Zebiak and Cane, 1987) to sophisticated coupled general circulation models.

The intermediate and complex models have been used for the ENSO predictions. Although some successes have been achieved, the prediction skill of ENSO is still low and cannot satisfy the requirement of preventing and reducing disaster. There are two main viewpoints for factors limiting ENSO forecast skill. One is that the model-based prediction of ENSO depends dominantly on the growth of initial error, which is based on the fact that ENSO is regarded as a self-sustaining oscillation (Chen et al., 1995; Thompson, 1998; Fan et al., 2000). Another competing viewpoint is that ENSO prediction depends on model errors, mainly unpredictable atmospheric noise, which describes ENSO as a linear stable or damped model triggered by stochastic forcing (Penland and Sardeshmukh, 1995; Thompson and Battisti, 2000; Fedorov et al., 2003). The issue of ENSO as a self-sustained oscillation mode or a stable mode triggered by stochastic

---

*Corresponding author: DUAN Wansuo, duanws@lasg.iap.ac.cn

forcing is presently not settled.

Many studies showed that more complete initialization procedures could significantly improve the predictability. Chen et al. (1995) designed a new initialization procedure that incorporated air-sea coupling in the ZC model and improved the model's forecast skill substantially. Chen et al. (1998) improved the ENSO prediction by assimilating observed sea level data in the model. Chen et al. (2004) used the LDEO5 version of the ZC model and successfully predicted all prominent El Niño events within the period 1857 to 2003 at lead times of up to two years. These suggested that El Niño might be controlled to a larger degree by self-sustaining internal dynamics than by stochastic forcing. The model-based prediction of El Niño may therefore depend much more on initial conditions than on the unpredictable atmospheric noise. Therefore, it is important to study the uncertainties of ENSO caused by initial errors (Mu et al., 2003; Duan and Mu, 2005). Naturally, we are required to answer the following questions: what kind of initial errors cause the severest prediction errors of ENSO? If data assimilation or (and) targeting observation approaches filter such kind of initial uncertainty, can the ENSO forecast skill be improved?

In Mu et al. (2003) and later Mu et al. (2007a), the authors utilized the approach of conditional nonlinear optimal perturbation (CNOP) to study the growth of initial errors for ENSO. The CNOP approach has also been employed by Duan et al. (2004) to study the optimal precursors of ENSO, and by Duan and Mu (2006) and Duan et al. (2008) to investigate the asymmetry of El Niño-La Niña. All these works show that CNOP is a useful tool to deal with these problems. Therefore, in this paper, CNOP approach will be used to address the above problems. Also, considering that Mu et al. (2007a) and Duan and Mu (2005) used a theoretical model, we will adopt the intermediate ZC model to investigate the initial error that causes the severest prediction uncertainty for ENSO.

2. Conditional nonlinear optimal perturbation

Let M_τ be the propagator of a nonlinear model from time 0 to τ. u_0 is an initial perturbation superimposed on the basic state $U(t)$, which is a solution to the nonlinear model and satisfies $U(t) = M_t(U_0)$ with U_0 being the initial value of basic state $U(t)$.

For a chosen norm $\|\cdot\|$, an initial perturbation $u_{0\delta}$ is called CNOP, if and only if

$$J(u_{0\delta}) = \max_{\|u_0\| \leqslant \delta} \|M_\tau(U_0 + u_0) - M_\tau(U_0)\|, \quad (1)$$

where $\|u_0\| \leqslant \delta$ is constraint condition of initial perturbations defined by the norm.

CNOP is the initial perturbation whose nonlinear evolution attains the maximal value of the objective function J at time τ (Mu et al., 2003; Mu and Zhang, 2006). But there exists a possibility that J attains its local maximum in a small neighborhood of a point in the phase space. Such an initial perturbation is called local CNOP. CNOP and local CNOP possess clear physical meanings. For example, in an anomaly model for ENSO, CNOP (local CNOP) superimposed on the climatological background state is most likely to evolve into an El Niño (La Niña) event and acts as the optimal precursors of El Niño (La Niña) events (Duan et al., 2004). In this situation, CNOP can be considered to be the most predictable, meaning that if this signal related to CNOP is observed in nature then the future outcome of the system is fairly certain. For the CNOPs superimposed on ENSO events, they describe initial errors that have the largest effect on the prediction results of ENSO.

CNOP and local CNOP can be calculated by the Spectral Projected Gradient Version 2 Method (SPG2) algorithm, which is used to solve the nonlinear minimization problems with equality or (and) inequality constraint conditions. The detailed description can be found in Birgin et al. (2000).

Although linear theory of singular vector (SV) has been widely applied to find the initial error of optimal growth related to ENSO predictability (Thompson, 1998; Fan et al., 2000; Samelson and Tziperman, 2001; Zhou et al., 2007), linear singular vector (LSV) is always associated with the sufficiently small initial perturbation and tangent linear model (TLM) (Oortwijin and Barkmeijier, 1995; Mu, 2000; Mu and Wang, 2001; Mu et al., 2003). It is limiting to use LSV to explore the initial error that has the largest effect on the prediction uncertainties. In the rest of this paper, we use CNOP to address this problem. It is expected that the nonlinear effect can be revealed.

3. Results

The ZC model is a well-known one and has been used in the study of prediction and predictability of ENSO extensively. The model describes the essential physics of ENSO, and thus provides a convenient tool for investigating the initial error that causes the severest prediction uncertainties of ENSO.

To find out the initial error pattern that causes the largest prediction error for SSTA, we follow Eq. (1) to construct the objective function related to CNOP as follows.

$$J(u_{0\delta}) = \max_{\|u_0\|_1 \leqslant \delta} \|T'(\tau)\|_2^2. \quad (2)$$

SSTA and thermocline depth anomaly are two important variables, which are coupled by upwelling. To consider what kind of initial error patterns of SSTA and thermocline depth anomaly yield the largest prediction uncertainties for SSTA, we choose the initial error $u_0 = (w_1 T_0', w_2 H_0')$, which is the non-dimensional initial errors of SSTA and thermocline depth anomaly vectors whose components are respectively the SSTA and thermocline depth anomaly on the different grids. w_1 and w_2 are the reciprocals of the characteristic scales of SSTA and thermocline depth anomaly whose values are taken as those in Wang and Fang (1996), that is, $w_1 = (2.0°\text{C})^{-1}$ and $w_2=(50 \text{ m})^{-1}$ and have been applied in Mu et al. (2007b). $\|u_0\|_1 \leqslant \delta$ is the constraint condition defined by the prescribed positive number δ and the norm $\|u_0\|_1 = \sqrt{\sum_{i,j}[(w_1 T_{0i,j}')^2 + (w_2 H_{0i,j}')^2]}$, where (i,j) represents a grid point in the region from 129.375°E to 84.375°W by grid spacing 5.625 degrees and from 19°S to 19°N by grid spacing 2 degrees. $T_{0i,j}'$ and $H_{0i,j}'$ denote respectively the dimensional initial errors of SSTA and thermocline depth anomaly at the grid point (i,j). The evolutions of these initial errors are measured by the norm $\|T'(\tau)\|_2 = \sqrt{\sum_{i,j}[w_1 T_{i,j}'(\tau)]^2}$. $T_{i,j}'(\tau)$ is obtained by subtracting SSTA of the reference state (i.e., "true state" to be predicted) at time τ from the predicted SSTA, and the latter is achieved by integrating the ZC model from time 0 to τ with the initial condition being the initial value of the reference state plus initial error u_0.

3.1   *CNOP-type errors of different reference states in ZC model*

Some reference states generated by integrating the ZC model are adopted as the "true states" to be predicted. Considering the different types of El Niño events in nature, we choose the reference states with an initial warm phase starting in January, April, July, and October, and denoted as $R_{\text{Jan}}^k, R_{\text{Apr}}^k, R_{\text{Jul}}^k$, and R_{Oct}^k, $k = 1, 2, 3, \ldots$ respectively. For these model El Niño events, the initial signals are very weak, even a negative SSTA (Niño-3 index; some examples are illustrated in Fig. 1). For each of these four different types of reference states, we choose many of them to perform the numerical experiments. Similar results are obtained. For simplicity, we choose the reference states with an initial time of January as the representatives to describe the results. Figure 1 shows the Niño-3 indices of these reference states denoted as $R_{\text{Jan}}^1, R_{\text{Jan}}^2, R_{\text{Jan}}^3$, and R_{Jan}^4. The reference state R_{Jan}^1 is a normal case, and the reference state $R_{\text{Jan}}^2, R_{\text{Jan}}^3$, and R_{Jan}^4 are El Niño events with different intensity
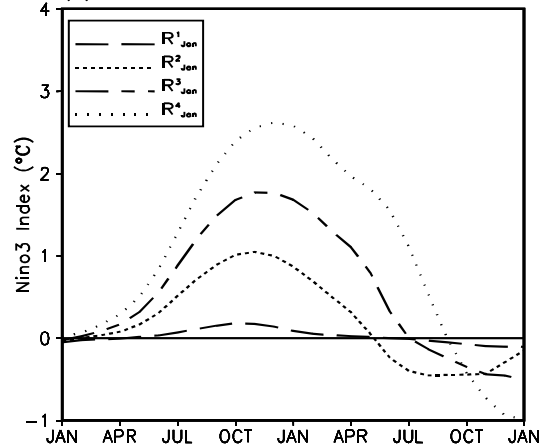

Fig. 1. The Niño-3 indexes of four reference states with initial time as January.

which tend to peak at the end of the year.

For the constraint bound $\delta \in [0.2, 1.2]$, we obtain the CNOPs of the above four reference states for a 12-month optimization period with an initial time of January, and explore the initial errors that have the largest effect on the prediction results. It is shown that the patterns of CNOP-type errors do not have obvious differences with the changing values of δ except for the grid values of the patterns. In Fig. 2, we show the patterns of CNOP-type errors of four reference states for initial constraint $\delta = 1.0$. It is easily seen that for the reference states R_{Jan}^1 and R_{Jan}^2, the SSTA component of CNOP-type errors consists of an east (positive)-west (negative) dipole spanning the entire tropical Pacific basin, and the thermocline depth anomaly component tends toward a deepening of the whole equatorial Pacific. But for reference states R_{Jan}^3 and R_{Jan}^4, CNOP-type errors have almost opposite characteristics, i.e., CNOP is of an east (negative)-west (positive) dipole of SSTA along the entire tropical Pacific basin, and the thermocline depth anomaly has a shoaling effect over the whole equatorial Pacific.

To address the dynamical growth of these CNOP-type errors for El Niño, we illustrate in Fig. 3 the prediction errors of four reference states caused by CNOPs, which are obtained by subtracting the Niño3 index of reference state from the predicted Niño3 index. From Fig. 3, it is easily demonstrated that the prediction error of reference states R_{Jan}^1 and R_{Jan}^4 are often larger than those of R_{Jan}^2 and R_{Jan}^3, which suggests that when the prediction is started in the months during which the signal in SSTA for El Niño is very weak (even a negative SSTA), it may be relatively difficult to predict normal state and strong El Niño events using the ZC model. The poor prediction of the ZC model of strong El Niño events may be one of its lim-
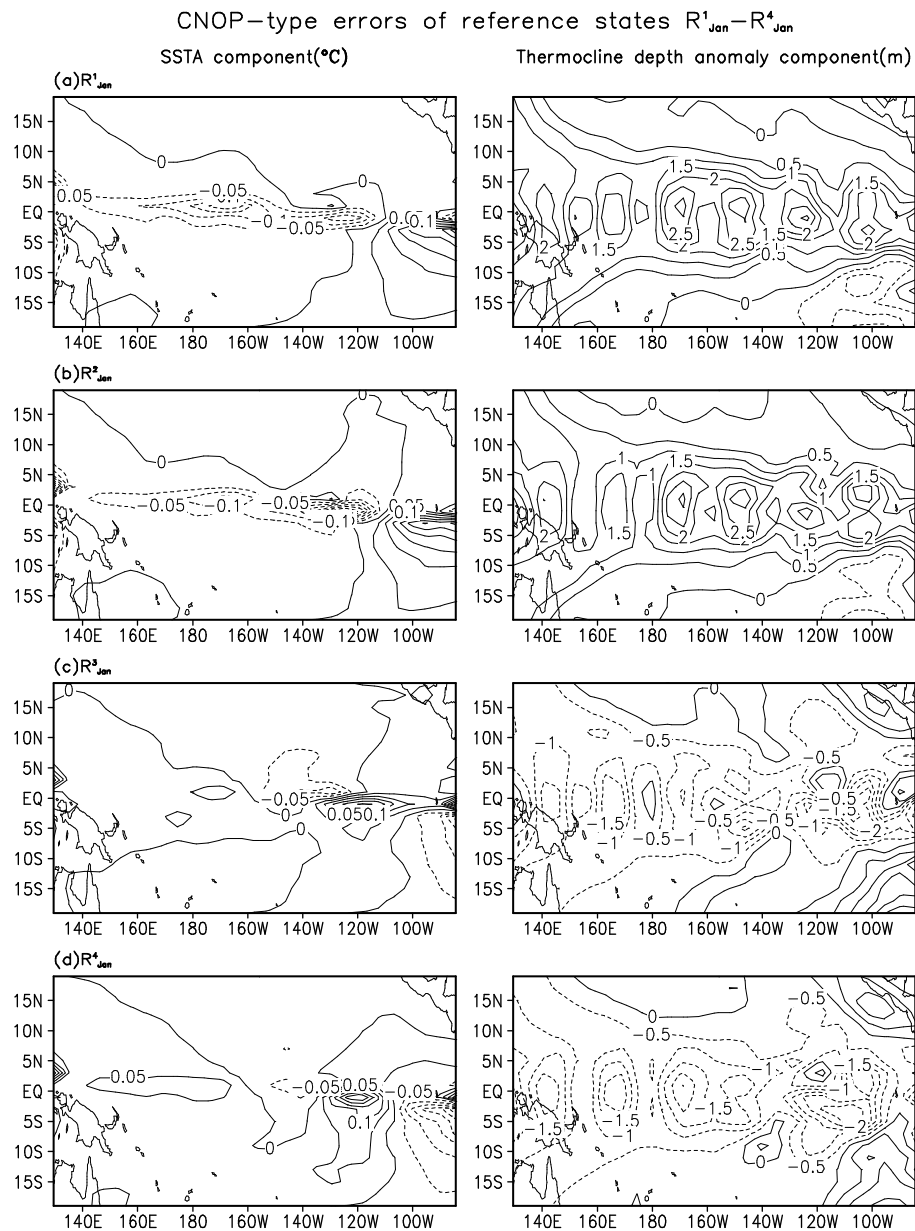
Fig. 2. The patterns of CNOP-type initial error with the magnitude of 1.0 (value of δ). In the left (right) column are SSTA (thermocline depth anomaly) components for reference state (a) R^1_{Jan}, (b) R^2_{Jan}, (c) R^3_{Jan}, and (d) R^4_{Jan}, respectively.

itations Liu and Duan (2008) used the hindcast data of the Lamont-Doherty Earth Observatory, Columbia University (LDEO) version 1 of the ZC model provided by the International Research Institute for Climate Prediction (IRI)/LDEO climate data library to investigate the error growth for El Niño events. They showed that the ZC model did not hit the strong 97/98 El Niño event when the prediction initialized in late October and January during which there were very weak signals, even negative SSTA. This supports the theoretical results in this paper.

In addition, by comparing the Niño-3 indices of reference state with those of the predicted, it is shown that the normal case R^1_{Jan} and the El Niño event R^2_{Jan} can be over-predicted and it tends to give a false alarm of El Niño prediction. For El Niño R^3_{Jan} and R^4_{Jan}, the ZC model tends to greatly underestimate the intensity of El Niño.

We also compute the LSV of the above reference states and compare their results with those of CNOP. Taking the initial conditions to be the initial values of the reference states plus the LSV-type errors, we
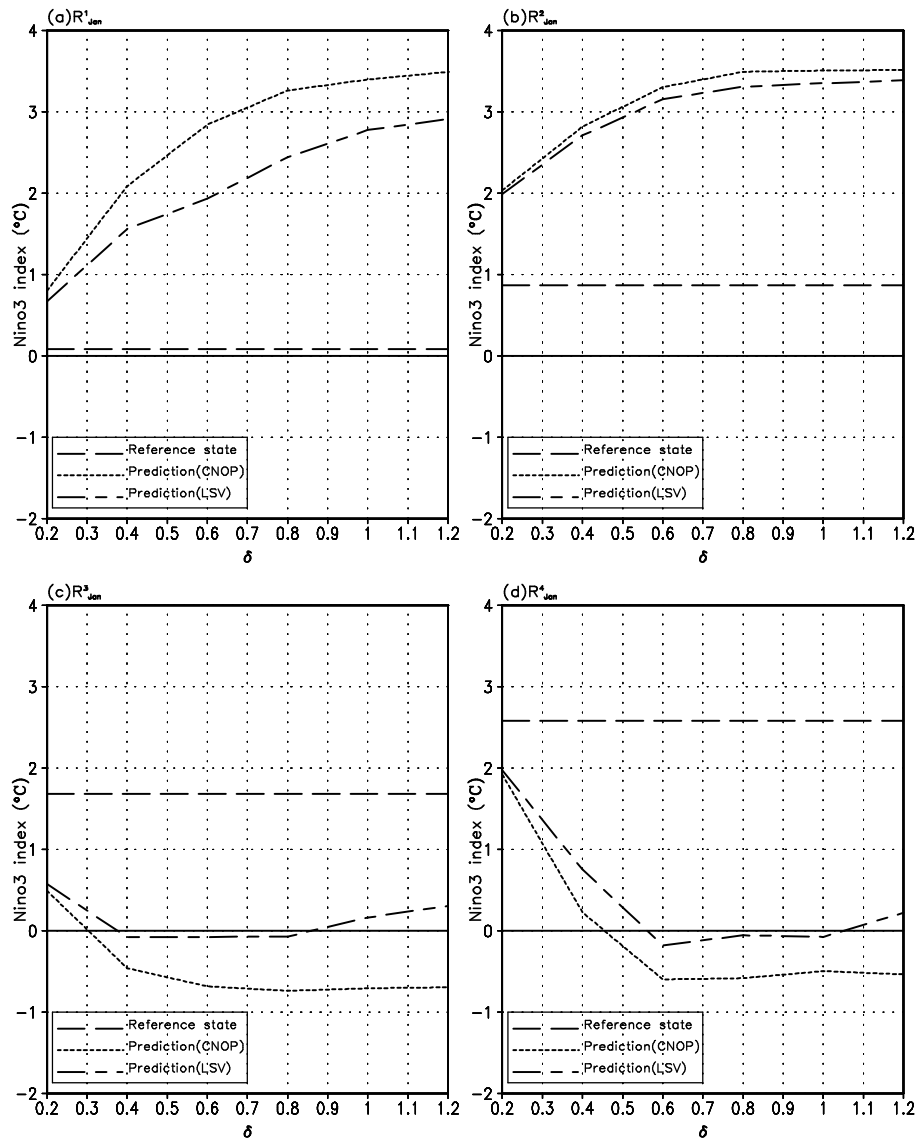
Fig. 3. The Niño-3 index of reference states (long-dashed line) and the predicted ones at the end of the optimization intervals as a function of δ (magnitude of initial error). The initial uncertainties in prediction are respectively CNOP (short-dashed line) and LSV (long-short-dashed line) type error. The reference states are the same as in Fig. 1.

integrate the ZC model for 12 months and obtain the predicted STA in December and then subtract the SSTA of reference states from the predicted SSTA. Thus, the growths of the LSV-type errors in the ZC model (not the tangent linear model of the ZC model) are obtained. It is demonstrated that when the initial errors are very small (values of δ), for example, δ = 0.2, the prediction errors caused by the LSV-type errors and CNOP-type errors have trivial difference. But for the large values of δ, the prediction errors caused by LSVs are always less than those caused by CNOP-type errors with the same magnitude as LSVs

(Fig. 3). That is, the LSV approach tends to underestimates the prediction uncertainties of ENSO in the ZC model. This result suggests that a CNOP-type error acts as the initial error that has the largest effect on the prediction results of ENSO. To further demonstrate this idea, we conduct another group of numerical experiments in next section.

3.2 Dependence of the prediction uncertainties on season and ENSO phase

In this section, we examine the dependence of ENSO prediction skill on phases of annual cycle and
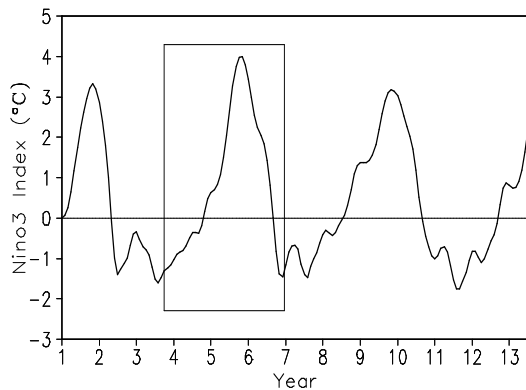
Fig. 4. The first 12-yr of the 100-yr time series of the SSTA in ZC model. The rectangle marks the chosen reference state—one El Niño event.

ENSO. During a 100-year time series of the control run Niño-3 index of the ZC model, about 23 El Niño events occur. Among these El Niño events, we choose several ENSO cycles to investigate the dependence of the error growth for El Niño events on the phases of El Niño itself and the seasonal cycle. For simplicity, we only describe the results of one of the El Niño events here. Figure 4 shows this El Niño event (where we only plot the time series of the first 12 years), which occurs during the period from model year 3 to model year 6. To explore the variability of ENSO prediction uncertainties, we consider the prediction error of this El Niño event caused by CNOP. The CNOPs of the chosen El Niño event are computed for 6 and 12 month optimization periods with start months as each month of the ENSO cycle, respectively. Because the chosen ENSO cycle spans model years 3–6, the start month that CNOP is superimposed on may be in different years. For convenience, we denote the different start months as "month (n)", where "month" represents the start month and "n" is the model year.

It is noticed that the El Niño events and the CNOP-type errors considered here are different from those in section 3.1, where we investigated the El Niño events with initial warm phase starting in different seasons and the CNOP-type errors superimposed on the initial months of those El Niño events. They are used to investigate the CNOP-type errors of the El Niño events with different intensities. But in this section, we consider an individual ENSO cycle, and the CNOP-type errors are superimposed on the different seasons of this ENSO cycle, which can be used to study the seasonality of error growth for ENSO.

Figure 5 shows the 6- and 12-month growths of CNOP-type errors as a function of start months for constraint condition 1.0. It is shown that for the 6-month optimization period (Fig. 5a), the prediction errors caused by CNOPs with start months Jan (5)

and May (4) are the largest. This can be explained as follows. The 6-month integrations starting from these two start months all include northern spring and summer. Furthermore, Jan (5) and May (4) are during the transition phase of ENSO from cold to warm. During this period, since El Niño signals are too weak to be captured, it easily yields the uncertainties. These uncertainties will grow aggressively during spring and summer due to the strong ocean-atmosphere couple instability (Mu et al., 2007a,b), and thus cause the largest error growth shown above. For the 12-month optimization period, the most severe prediction uncertainty is caused by CNOP with a start month of Dec (4), which is also during the transition period of ENSO. All of these results suggest that it may be the most difficult when the ENSO prediction is made at the transition phase and bestriding northern spring. It is also indicated that the skill of ENSO forecasts may depend on the phases of annual cycle and ENSO.

To investigate the effect of nonlinearity on error growth of ENSO, we also illustrate the results of LSV in Fig. 5. It is demonstrated that there are considerable differences between the growth of CNOP and that of LSV, although CNOP and LSV have the same magnitude as measured by norm. The nonlinear evolution of CNOP tends to be larger than that of LSV, especially for the long optimization period (Fig. 5b). These results show that the LSV approach underestimates error growth and has limitations in evaluating the predictability of ENSO. From this result, we infer that ENSO forecast skill depends on the types of initial error. CNOP-type error is the initial error that causes the most severe prediction uncertainties for ENSO.

4.   Summary and discussion

Within the frame of the Zebiak-Cane model (ZC model), we use the approach of conditional nonlinear optimal perturbation (CNOP) to investigate the initial error that has the largest effect on prediction results of ENSO and its dynamic behavior. It is demonstrated that CNOP-type errors have the largest negative effect on ENSO forecasts. We find that for the different reference states (including El Niño events) in the ZC model, the initial error may have different dynamical growth. For the normal states and the relatively weak El Niño events considered in this paper, the ZC model tends to give false alarms of ENSO prediction. For the relatively strong El Niño events in the ZC model, the model tends to underestimate the intensities. Also, our results demonstrate that the error growth for El Niño events in the ZC model is sensitive to the phase of annual cycle and El Niño itself. The prediction as made in transition phase and bestriding northern spring and summer may have low
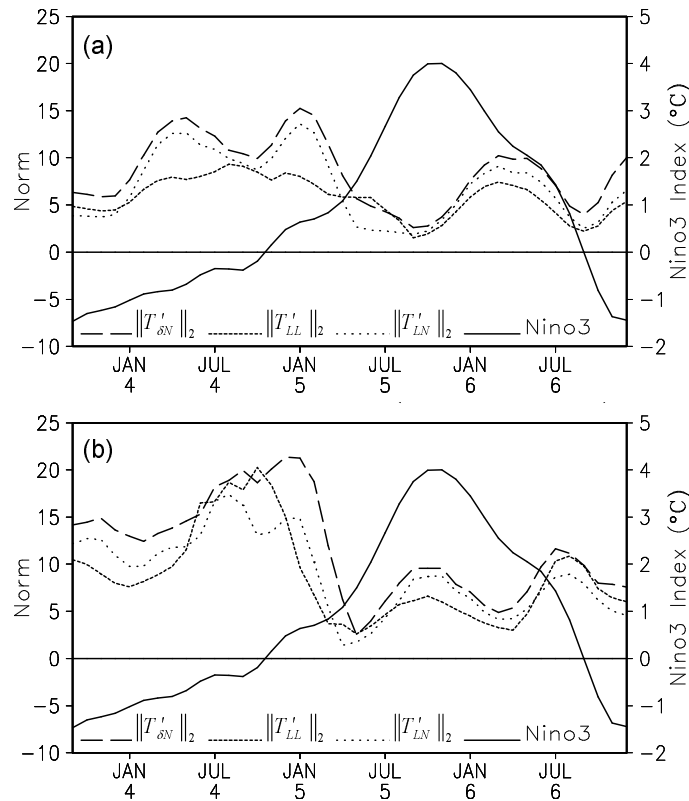
Fig. 5. The 6-month (a) and 12-month (b) evolutions of CNOPs and LSVs as a function of the start times. The long-dashed line denotes the nonlinear evolution $\|T'_{\delta N}\|_2$ of CNOP. The short-dashed (dotted) line represents the linear (nonlinear) evolution $\|T'_{LL}\|_2$ ($\|T'_{LN}\|_2$) of LSV. The solid line is the Niõ-3 index of the ENSO cycle chosen in Fig. 4.

forecast skill. This indicates that the condition during northern spring and summer is favorable for the error growth of ENSO.

Although linear singular vector (LSV) is also a useful approach in estimating ENSO prediction uncertainties, our results suggest that LSV tends to underestimate the prediction uncertainties of ENSO in the ZC model. This indicates that the different types of initial errors may cause the different amplitudes of prediction uncertainties of ENSO, although the magnitudes of initial errors are the same. CNOP-type error acts as the initial error that has largest negative effect on prediction results of ENSO.

The above results demonstrate that ENSO prediction is closely related to the accuracy of the initial fields. This implies that if the CNOP-type error can be filtered by a proper data assimilation method, the prediction skill of ENSO may be improved. Also, if the spatial patterns of CNOPs of El Niño are well localized they might represent the "sensitive area" of error, which suggests that intensifying observations in these "sensitive area" might be important to increase the

ENSO forecast skill.

The results in this paper were derived from the simple ZC model. And the prediction uncertainties for ENSO events were only evaluated by measuring the growth of initial error. That is to say, this study falls in a "perfect model scenario". The obtained results are therefore indicative. It is expected that the future works can address the following issues: the first question is whether the results obtained in this paper is model-dependent; the second question is whether the results in this paper depend on the chosen measurement of predictability; third, are the prediction uncertainties for ENSO reported by other papers (e.g. Chen et al., 2004; Tang et al., 2005) caused only by initial errors? All of these questions deserve our future studies.

REFERENCES

Battisti, D. S., and A. C. Hirst, 1989: Interannual variability in the tropical atmosphere/ocean system: influences of the basic state, ocean geometry and nonlinearity. *J. Atmos. Sci.*, **46**, 1687–1712.

Birgin, E. G., J. M. Martínez, and M. Raydan, 2000: Nonmonotone Spectral Projected Gradient Methods on Convex Sets. Society for Industrial and Applied Mathematics. *Journal on Optimaization*, **10**, 1196–1211.

Cane, M. A., S. E. Zebiak, and S. C. Dolan, 1986: Experimental forecasts of El Niño. *Nature*, **321**, 827–832.

Chen, D., S. E. Zebiak, A. J. Busalacchi, and M. A. Cane, 1995: An improved procedure for El Niño forecasting: Implications for predictability. *Science*, **269**, 1699–1702.

Chen, D. K., M. A. Cane, S. E. Zebiak, and A. Kaplan, 1998: The impact of sea level data assimilation on the Lamont model prediction of the 1997/98 El Niño. *Geophys. Res. Lett.*, **25**, 2837–2840.

Chen, D., M. A. Cane, A. Kaplan, S. E. Zebiak, and D. J. Huang, 2004: Predictability of El Niño over the past 148 years. *Nature*, **428**, 733–736.

Duan, W. S., and M. Mu, 2005: Applications of nonlinear optimization methods to quantifying the predictability the predictability of a numerical model for El Niño-Southern Oscillation. *Progress in Natural Science*, **15**, 915–921.

Duan, W. S., and M. Mu, 2006: Investigating decadal variability of El Niño-Southern Oscillation asymmetry by conditional nonlinear optimal perturbation. *J. Geophys. Res.*, **111**, C07015, doi:10.1029/2005JC003458.

Duan, W. S., M. Mu, and B. Wang, 2004: Conditional nonlinear optimal perturbations as the optimal precursors for El Niño-Southern Oscillation events. *J. Geophys. Res.*, **109**, D23105, doi: 10.1029/2004JD004756.

Duan, W. S., H. Xu, and M. Mu, 2008: Decisive role of nonlinear temperature advection in El Niño and La Niña amplitude asymmetry. *J. Geophys. Res.*, **113**, C01014, doi:10.1029/2006JC003974.

Fan, Y., M. R. Allen, D. L. T. Anderson, and M. A. Balmaseda, 2000: How predictability depends on the nature of uncertainty in initial conditions in a coupled model of ENSO. *J. Climate*, **13**, 3298–3313.

Fedorov, A. V., S. L. Harper, S. G. Philander, B. Winter, and A. Wittenberg, 2003: How Predictable is El Niño? *Bull. Amer. Meteor. Soc.*, **84**, 911–919.

Jin, F. F., 1997: An equatorial ocean recharge paradigm for ENSO. Part I: Conceptual model. *J. Atmos. Sci.*, **54**, 811–829.

Liu, X. C., and W. S. Duan, 2008: Analysis of the predictability of Zebiak-Cane ENSO model. *Climatic and Environmental Research*, in press. (in Chinese)

Mu, M., 2000: Nonlinear singular vectors and nonlinear singular values. *Science in China* (*D*) , **43**, 375–385.

Mu, M., and J. C. Wang, 2001: Nonlinear fastest growing perturbation and the first kind of predictability. *Science in China* (*D*), **44**, 1128–1139.

Mu, M., and Z. Y. Zhang, 2006: Conditional nonlinear optimal perturbation of a barotropic model. *J. Atmos. Sci.*, **63**, 1587–1604.

Mu, M., W. S. Duan, and B. Wang, 2003: Conditional nonlinear optimal perturbation and its applications. *Nonlinear Processes in Geophysics*, **10**, 493–501.

Mu, M., W. S. Duan, and B. Wang, 2007a: Season-dependent dynamics of nonlinear optimal error growth and El Niño-Southern Oscillation predictability in a theoretical model. *J. Geophys. Res.*, **112**, D10113, doi:10.1029/2005JD006981.

Mu, M., H. Xu, and W. Duan, 2007b: A kind of initial errors related to "spring predictability barrier" for El Niño events in Zebiak-Cane model. *Geophys. Res. Lett.*, **34**, L03709, doi:10.1029/2006GL027412.

Oortwijin, J., and J. Barkmeijier, 1995: Perturbations that optimally trigger weather regimes. *J. Atmos. Sci.*, **52**, 3932–3944.

Penland, C., and P. D. Sardeshmukh, 1995: The optimal growth of tropical sea surface temperature anomalies. *J. Climate*, **8**, 1999–2024.

Samelson, R. M., and E. Tziperman, 2001: Instability of the chaotic ENSO: The growth-phase predictability barrier. *J. Atmos. Sci.*, **58**, 3613–3625.

Tang, Y. M., R. Kleeman, and A. Moore, 2005: On the reliability of ENSO dynamical predictions. *J. Atmos. Sci.*, **62**, 1770–1791

Thompson, C. J., 1998: Initial conditions for optimal growth in a coupled ocean-atmosphere model of ENSO. *J. Atmos. Sci.*, **35**, 537–557.

Thompson, C. J., and D. S. Battisti, 2000: A linear stochastic dynamical model of ENSO, Part I: Model development. *J. Climate*, **13**, 2818–2832.

Wang, B., and Z. Fang, 1996: Chaotic oscillations of tropical climate: A dynamic system theory for ENSO. *J. Atmos. Sci.*, **53**, 2786–2802.

Zebiak, S. E., and M. A. Cane, 1987: A model El Niño Southern Oscillation. *Mon. Wea. Rev.*, **115**, 2262–2278.

Zhou, X. B., Y. M. Tang, and Z. W. Deng, 2007: The impact of atmospheric nonlinearities on the fastest growth of ENSO prediction error. *Climate Dyn.*, DOI: 10.1007/s00382-007-0302-5.